



Amperometric Biosensor for the Detection of *Enterobacter aerogenes* as Biological Weapon

Harish Kumar* and Bhawana

Material Science and Electrochemistry Lab., Department of Chemistry, Ch. Devi Lal University, Sirsa, Haryana - 125 055. (India).

ARTICLE INFO

Article history:

Received: 25 November 2015;

Received in revised form:

3 January 2016;

Accepted: 9 January 2016;

Keywords

Biological Warfare Agents,
Biosensors,
Sol-Gel Method,
Fe₃O₄ Nanoparticles,
Enterobacter Aerogenes.

ABSTRACT

A carbon based (Graphene) working electrode containing enzyme alkaline phosphatase, cellulose acetate and Poly Vinyl Pyrolidone (PVP), Ferrocene, Horseradish peroxidase and aq. KOH was specially designed and fabricated. It is then combined with Ag/AgCl reference and a platinum electrode to form three electrodes based amperometric biosensor for the electrochemical detection of *Enterobacter aerogenes* as biological warfare agent (BWA) in the presence and absence of Fe₃O₄ nanoparticles. Fe₃O₄ nanoparticles were synthesized by sol-gel technique and were characterized by UV-visible, FTIR, TEM and XRD techniques. Change in current response and OCP values helps in the detection of BWA in presence and absence of Fe₃O₄ nanoparticles. Effects of temperature, stirring and Fe₃O₄ nanoparticles on the BWA have also been investigated.

© 2016 Elixir All rights reserved.

Introduction

Bioterrorism is the use of a biological weapon (bacteria, virus or spores) on human life as a weapon of mass infection. It ultimately proves more powerful than a chemical or a nuclear weapon because it works silently and its effects can be far-reaching and uncontrollable. List of pathogenic bacteria that can be considered as possible biological warfare agents is unending [1]. Highly dangerous include *Botulinum toxin*, *Francisellatularensis*, *Salmonella typhimurium*, *Staphylococcus epidermis*, *Enterobacter aerogenes* and *Yersinia pestis*. Other bio-agents, like *Venezuelan equine encephalitis*, *Marburg*, *Ebola*, and influenza viruses are of lesser importance, despite the fact, that infections with these viruses are serious and mortality is relatively high, but due to the difficulty in their preparation, their position on the list of Biological Warfare Agents (BWA) is lower. First evidence of bioterrorism came in to existence in 1979, when doctors presented a report of mass civilian death due to *B. anthracis* pneumonia i.e. due to inhalation of anthrax. A person exposed to *B. anthracis* died immediately. The bacilli of anthracis multiply rapidly in the body and produce a harmful toxin that stops the process of breathing.

Similarly, *Enterobacter aerogenes* is a nosocomial and pathogenic bacterium that causes opportunistic infections. Infections commonly attributed to *E. aerogenes* are respiratory, gastrointestinal, and urinary tract infections, specifically cystitis, in addition to wound, bloodstream, and central nervous system infections. The National Pharmaceutical Stockpile Program (NPS) is designed to enable such a response to a bioterrorist attack. In comparison with chemical warfare agents (CWA), BWA production is much cheaper and terrorist or military attack with BWA is more effective in the range of hazard area and in the number of expected casualties. The infectious dose (ID) (amount of organism needed for infection outbreak) is different for every

agent. Usually the intake of aerosol (particles 1 - 10 μm) through lung is able to evocate disease with a lower ID for the given BWA.

Different types of electrochemical biosensors which are in common practice are: Potentiometric, conductometric, amperometric, and impedimetric [2-5]. Out of these, amperometric biosensors are more common in practice and are usually based on ion-selective electrodes. These are three electrode based electrochemical systems which are attached with electrochemical detectors which measure the changes in ion concentration during reaction taking place in the bio-recognition layer. The advantage of Amperometric biosensors over other biosensors is that they are highly sensitive, rapid, linear concentration dependence and inexpensive [6]. Amperometric biosensors aimed at microbial analysis have been reported by different researchers [7-11]. First biosensors used pH glass electrode with enzymes captured in a suitable membrane. In potentiometric immune-sensor electrochemical biosensor, enzyme-labeled antibodies are used. The most common labeling enzymes are urease, glucoseoxidase or alkaline phosphatase, which are able to change either pH or ionic strength in the course of the detection [12]. Very popular semiconductor-based biosensors are light-addressable potentiometric sensors (LAPS). Due to their small size and possible multichannel arrangement, these devices seem to be very convenient for simultaneous analysis of several analytes [13]. The LAPS immune-sensors were used to detect *Francisellatularensis* [14] with a limit of detection (LOD) at 3.4×10^3 cells/ml and *Bacillus melitensis* with LOD equal to 6×10^3 cells/ml during the 1h incubation time [15]. A better LOD was achieved for *Escherichia coli* DH5 a strain [16]; the secondary antibody specific against *Escherichia coli* labeled with urease was used and LOD of 10 cells/ml for 1.5 h assay time was claimed.

In continuation to our earlier study [17], current research is focused on the fabrication of electrochemical biosensor for the detection of *Enterobacter aerogenes* as biological warfare agent.

Materials and Methods

Samples of disease causing bacteria i.e. *Enterobacter aerogenes* (MTCC 2822) were collected from Microbial Type Culture Collection (MTCC), Institute of Microbial Technology, Chandigarh.

Different steps used for the electrochemical determination of disease causing bacteria are:

Preparation of Bacterial Strain

The bacterial test organism *Enterobacter aerogenes* was grown in nutrient broth for 24 hours at 37 °C. A sodium phosphate buffer solution of pH 7.0 was prepared to hold these disease causing bacteria at a very low temperature i.e. 4 °C.

Synthesis of Fe₃O₄ Nanoparticles and Graphene

Fe₃O₄ nanoparticles were synthesized by Sol-gel technique. In this technique, metal salt solution having Ferric chloride is added drop wise in a mixture of tetraethyl orthosilicate in ethanol. Reduced graphene was synthesized by well known Hummers method.

Characterization of Fe₃O₄ Nanoparticles and Graphene

Characterization of Fe₃O₄ nanoparticles and Graphene was carried out by using UV-visible spectroscopy, Fourier Transform Infra-Red (FT-IR) technique, X-ray diffraction (XRD) study and Transmission Electron Microscopy (TEM) techniques.

Fabrication of Working Test Electrode

A carbon paste (Graphene) working electrode was fabricated for the electrochemical determination of biological weapon. A slurry was prepared by mixing reduced Graphene, alkaline phosphatase, cellulose acetate, Ferrocene, Horseradish Peroxidase, aq. KOH and Poly vinyl pyrrolidone (PVP). This slurry was filled in working test electrode with the help of luggin capillary. A copper wire is dipped from outside in the slurry for making electrical connections.

Fabrication of Three electrodes based Electrochemical Biosensor

A three electrodes based electrochemical cell was fabricated having three electrodes i.e. a working test electrode (cellulose acetate, PVP bound carbon paste electrode), Ag/AgCl reference electrode and a platinum electrode acting as an auxiliary electrode for the electrochemical determination of disease causing pathogen (Figure 1).

Electrochemical Characterization

Three electrodes based electrochemical biosensor is connected to the instrument electrochemical workstation PGSTAT 128N, Metrohm Autolab attached to a PC and digital controlled water bath to maintain constant temperature. Electrochemical measurement experiment were performed on a pathogenic bacteria *Enterobacter aerogenes* and change in Open Circuit Potential (OCP), current (nA) and potential values were recorded at different conditions.

For the electrochemical characterization, 3×10^7 CFU of *Enterobacter aerogenes* in 50 ml of PBS buffer solution was used. Four different samples were prepared i.e. pure PBS buffer solution as sample 1, PBS buffer solution with 3×10^7 CFU of *Enterobacter aerogenes* as sample 2, PBS buffer solution with Fe₃O₄ nanoparticles as sample 3 and PBS buffer solution with Fe₃O₄ nanoparticles and 3×10^7 CFU of *Enterobacter aerogenes* as sample 4.

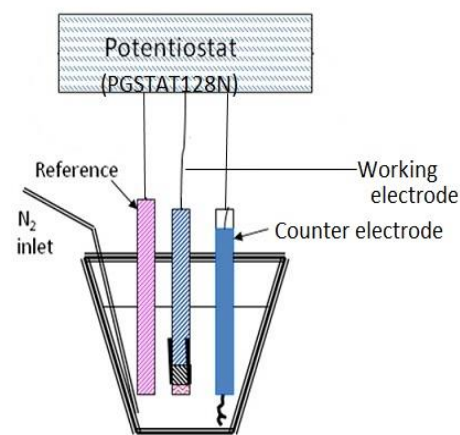


Figure 1. Electrochemical biosensor for the detection of biological warfare agent.

The above samples were kept under following two observations:

- Heating at a constant temperature of 70 °C without stirring for 6 hours.
- Continuous stirring for 6 hours at room temperature.

After 6 hours, we have recorded the current and potential values with the help of three electrodes based electrochemical cell connected to the instrument PGSTAT 128N, Metrohm Autolab.

Results

Result of electrochemical characterization on *Enterobacter aerogenes* is recorded in the form of Tables 1 and 2 and Figures 2-5. Table 1 shows OCP values of unstirred and stirred samples (06 hours of continuous stirring). Table 2 shows the OCP values of four different heated samples at initial time and after 6 hours.

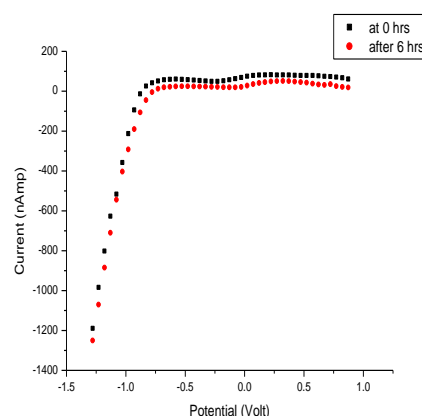


Figure 2. Current and potential behaviour of pure PBS buffer solution at 0.0 and after 6.0 hours of stirring.

Figure 2 shows current and potential values of pure PBS buffer solution at 0.0 and after 6.0 hours. Figure 3 shows current and potential behavior of PBS buffer solution in presence of *Enterobacter aerogenes* at 0.0 and after 6.0 hours. Figure 4 shows current and potential behavior of PBS buffer solution in presence of Fe₃O₄ nanoparticles (50 µl/ml) at 0.0 and after 6.0 hours. Figure 5 shows current and potential behavior of PBS buffer solution in presence of *Enterobacter aerogenes* and Fe₃O₄ nanoparticles (50 µl/ml) at 0.0 and after 6.0 hours.

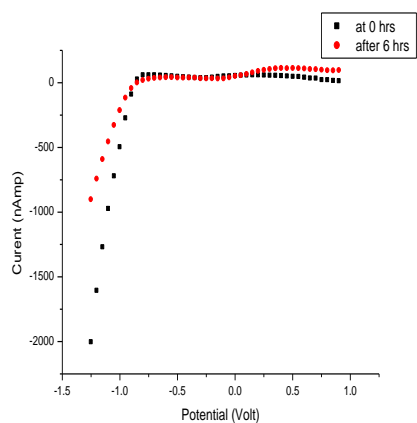


Figure 3. Current versus potential behavior of PBS buffer solution in presence of Fe_3O_4 nanoparticles (50 $\mu\text{l}/\text{ml}$) at 0.0 and after 6.0 hours of stirring.

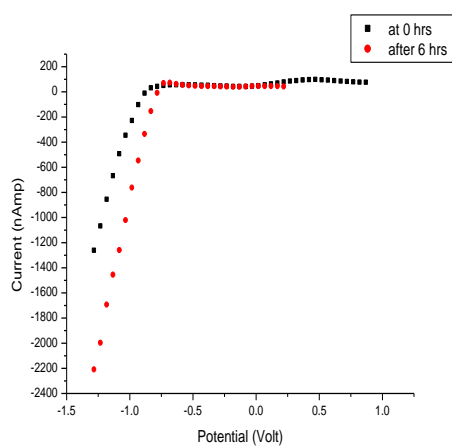


Figure 4. Current versus potential behavior of PBS buffer solution with *Enterobacter aerogenes* at 0.0 and after 6.0 hours of stirring.

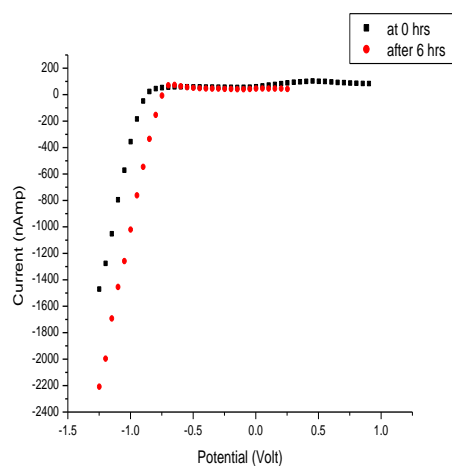


Figure 5. Current versus potential behavior of PBS buffer solution in presence of *Enterobacter aerogenes* and Fe_3O_4 nanoparticles (50 $\mu\text{l}/\text{ml}$) at 0.0 and after 6.0 hours of stirring.

Figure 6 shows current and potential values of pure PBS buffer solution at 0.0 and after 6.0 hours of heating at 70.0°C . Figure 7 shows current and potential behavior of PBS buffer solution in presence of *Enterobacter aerogenes* at 0.0 and after 6.0 hours of heating at 70.0°C . Figure 8 shows current

and potential behavior of PBS buffer solution in presence of Fe_3O_4 nanoparticles (50 $\mu\text{l}/\text{ml}$) at 0.0 and after 6.0 hours of heating at 70°C .

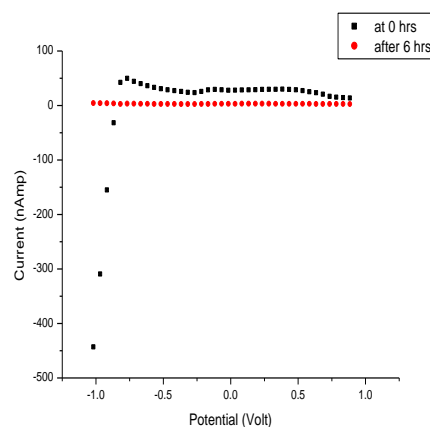


Figure 6. Current and potential behavior of pure PBS buffer solution at 0.0 and after 6.0 hours of heating.

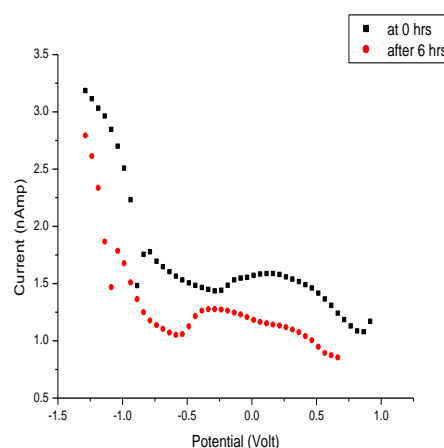


Figure 7. Current versus potential behavior of PBS buffer solution in presence of Fe_3O_4 nanoparticles (50 $\mu\text{l}/\text{ml}$) at 0.0 and after 6.0 hours of heating.

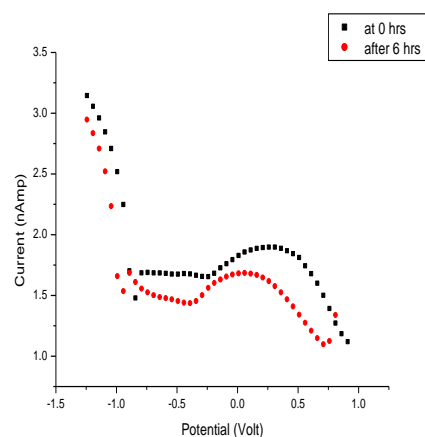


Figure 8. Current versus potential behavior of PBS buffer solution with *Enterobacter aerogenes* at 0.0 and after 6.0 hours of heating.

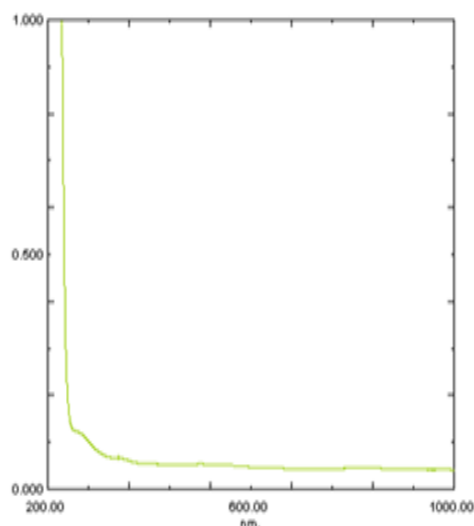


Figure 9. UV-Visible spectra of Fe₃O₄ nanoparticles.

Figure 9 shows UV-visible spectra of Fe₃O₄ metal nanoparticles synthesized by sol-gel technique as a function of wavelength.

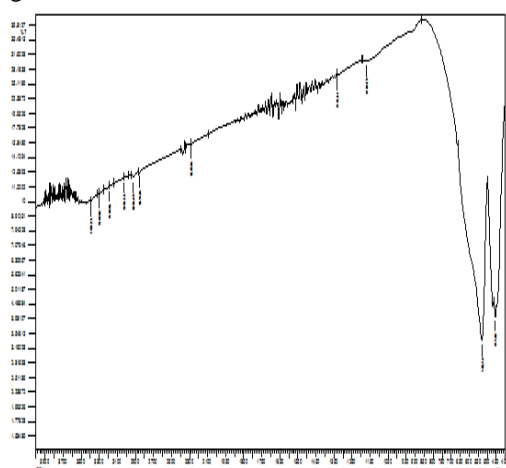


Figure 10. FT-IR spectra of Fe₃O₄ nanoparticles.

Figure 10 shows Fourier Transform Infra-Red (FT-IR) spectra (Thermo-USA, FTIR-3800) in the wavelength range of 400 - 4000 cm⁻¹ of Fe₃O₄ metal nanoparticles synthesized by sol-gel technique.

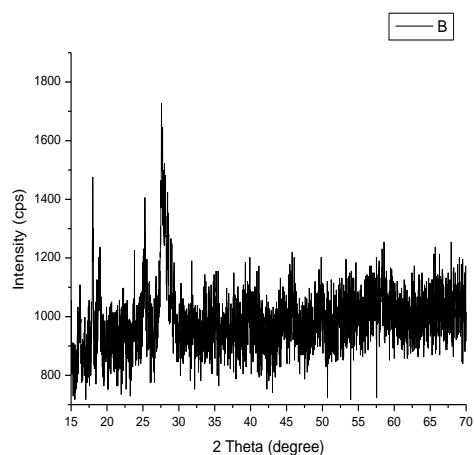


Figure 11. XRD diffraction pattern of Fe₃O₄ nanoparticles.

Figure 11 shows XRD pattern of Fe₃O₄ metal nanoparticles synthesized by sol-gel technique. Figure 12 shows TEM images of Fe₃O₄ metal nanoparticles synthesized by sol-gel technique.

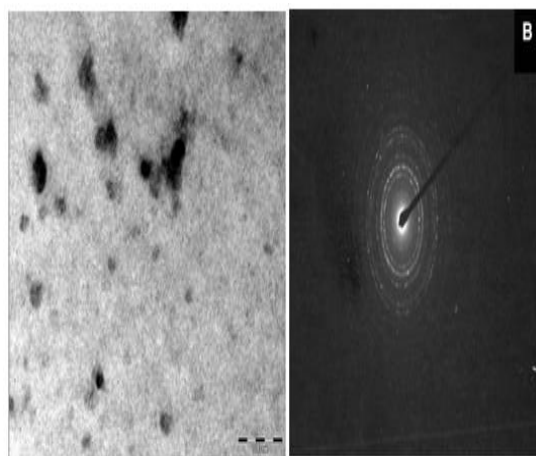


Figure 12. (a) TEM images of Fe₃O₄ nanoparticles (b) Diffraction pattern of Fe₃O₄ nanoparticles.

Discussion

The UV absorption band of Fe nanoparticles (Figure 9) was observed in the wavelength range of 330–450 nm which may be due to the absorption and scattering of light by iron nanoparticles [18-19]. The low absorption band at a wavelength of 410 nm may be due to the formation of least agglomerated Fe₃O₄ nanoparticles. Further, no additional peaks were observed corresponding to alcohol which indicates that the iron nanoparticles were not encapsulated by ethanol and they only acted as a soft template.

An absorption peak at 3,440 cm⁻¹ in the FTIR spectrum of iron oxide nanoparticles (Figure 10), (characteristic peak of OH stretching vibration) confirms the presence of some amount of ferric hydroxide in Fe₃O₄[20-21]. The other two distinct peaks at 565 and 421 cm⁻¹ are due to the vibrations of Fe²⁺-O²⁻ and Fe³⁺-O²⁻ respectively [22]. Another peak (sharp and high intensity) at 565 cm⁻¹ indicates the presence of high degree of crystallinity in the Fe₃O₄ nanoparticles. The characteristic absorption bands at 565 and 421 cm⁻¹ confirms the presence of spinel structure in Fe₃O₄ nanoparticles. FT-IR spectroscopic technique was carried out in order to ascertain the purity and nature of ferrite metal nanoparticles synthesized by sol-gel technique.

The reflection peak at 2θ = 35.60° confirm spinel phase of ferrite (Fe₃O₄) nanoparticles (JCPDS, PDF cards 3-864 and 22-1086) (Figure 8). The diffractions peaks of the ferrite nanoparticles were observed at 2θ = 30.18° (d = 0.297 nm), 35.61° (d = 0.253 nm), 43.27° (d = 0.209 nm), 53.56° (d = 0.171 nm) and 57.11° (d = 0.162 nm) [23]. The peaks at an angle of 30.18° (220), 35.612° (311), 43.278° (400), 53.569° (422), 57.118° (511) and 62.655° (440) correspond to Fe₃O₄. The average particle size of ferrite nanoparticles has been calculated using well known Scherrer equation [24] and was found to be 31.0 nm. Further, diffraction peak broadening confirms the formation of the ultrafine ferrite nanoparticles.

Structural and optical properties of Fe₃O₄ metal nanoparticles were determined by using Transmission Electron Microscope (TEM) of made Morgagni 268 D, FEI Philips at a resolution of 2 Å from Electron Microscope Facility (SAIF), AIIMS, New Delhi (Figure 12). The TEM images reveals self-organized network like morphology of ferrite (Fe₃O₄) nanoparticles which are almost identical in shape and appear to be uniformly dispersed. The average particles size is in close agreement with both the technique i.e. as observed in TEM and the crystallite size calculated by the Scherrer equation (~31.0 nm) with the help of XRD technique.

Further, the TEM diffraction ring (Figure 12 b) confirms that the ferrite nanoparticles are in a well crystalline state [25].

Purpose of addition of Horseradish peroxidase (HRP) in the slurry of working electrode is because HRP enhance the intensity of weak electrochemical signal. Ferrocene act as stimulator. Grapheme was added in to the slurry of working electrode in order to increase its conductivity and surface area of the electrode.

Table 1. Open Circuit Potential (OCP) values of Stirred samples of *Enterobacter aerogenes*.

Sr. No.	Samples	OCP Values(Volt)at0 and 6.0 hours	
1.	Pure PBS solution	0.524	0.545
2.	PBS solution with Fe ₃ O ₄ nanoparticles	0.747	0.753
3.	PBS solution with 3.0 × 10 ⁷ CFU of <i>Enterobacter aerogenes</i>	0.778	0.854
4.	PBS solution with Fe ₃ O ₄ nanoparticles and 3.0 × 10 ⁷ CFU of <i>Enterobacter aerogenes</i>	0.743	0.589

Table 2. Open Circuit Potential (OCP) values of heated samples of *Enterobacter aerogenes*.

Sr.No.	Samples	OCP Values(Volt)at0 and 6.0 hours	
1.	Pure PBS solution	0.514	0.553
2.	PBS solution with Fe ₃ O ₄ nanoparticles	0.782	0.551
3.	PBS solution with 3.0 × 10 ⁷ CFU of <i>Enterobacter aerogenes</i>	0.738	0.649

From the Tables 1 and 2, it is observed that OCP value increases on addition of Fe₃O₄ nanoparticles (50 µl/ ml) and 3.0 × 10⁷ CFU of *Enterobacter aerogenes*. It means that addition of Fe₃O₄ nanoparticles increases the conductivity of the medium and hence results into increase in OCP value. Heating of sample No. 1 to 70.0 °C leads to increase in the OCP value from 0.514 to 0.553 V. Heating of sample no. 3 to 70.0 °C makes *Enterobacter aerogenes* inactive which lowers its OCP value. It is observed from the Table 1 that the addition of Fe₃O₄ nanoparticles (50 µl/ml) at room temperature in the sample containing 3.0 × 10⁷ CFU of *Enterobacter aerogenes* results into slight decrease in OCP value.

It is observed from Table 2 that heating of sample no. 3 to 70.0 °C for 6.0 hours results in decrease in OCP value from 0.738 to 0.649 V. Hence, it is observed that an OCP value of 0.524 V in phosphate buffer solution confirms the presence of *Enterobacter aerogenes* pathogenic bacteria. Heating of the samples up to 70.0 °C for a definite period of time leads to decrease in OCP value. Addition of Fe₃O₄ nanoparticles also leads to slight decrease in OCP value i.e. heating of sample makes bacteria inactive which results in the decrease in OCP value.

It is observed from Fig. 2 that the current and potential behavior of pure PBS solution remains almost same at 0.0 and 6.0 hours of continuous stirring. Value of current first increase sharply with increase in potential value and then remains almost constant with increase in potential value. It is observed from Fig. 3 that there is deviation in current value at smaller value of potential of PBS buffer solution in presence of Fe₃O₄ nanoparticles (50 µl/ ml) at 0.0 and after 6.0 hours of continuous stirring. But at higher potential value current and potential behavior of pure PBS solution remains almost same. Similar results were observed in case of samples containing *Enterobacter aerogenes*(Figure 4). Similar results were observed in case of samples containing both Fe₃O₄

nanoparticles (50 µl/ ml) and 3.0 × 10⁷ CFU of *Enterobacter aerogenes* (Figure 5).

It is observed from the Fig. 6 that the value of current first increases and then remains almost constant with increase in potential value at room temperature. But after heating of the samples to 70.0 °C, the current value remains constant and become independent of potential value. It is observed from the Fig. 7 that the value of current continuously decreases with increase in potential value in presence of Fe₃O₄ nanoparticles at 70.0 °C temperature. Figure 8 shows that value of current continuously decreases with increase in potential value in presence of 3.0 × 10⁷ CFU of *Enterobacter aerogenes* in PBS solution at 70.0 °C. The decrease in current value at smaller value of potential is high and at a high potential decrease in current value is small.

Conclusion

A carbon (Graphene) based working electrode having alkaline phosphatase, cellulose acetate, Ferrocene, Horseradish peroxidase, aq. KOH and PVP was fabricated which when combined with Ag/AgCl reference and a platinum auxiliary electrode to form a three electrode based electrochemical cell for the electrochemical detection of *Enterobacter aerogenes* as biological warfare agent. Fe₃O₄ nanoparticles were synthesized by sol-gel method. Characterization of Fe₃O₄ nanoparticles was carried out by using UV-visible, FT-IR, XRD and TEM techniques. An UV-visible absorption band at the wavelength of 410 nm and a sharp absorption band at 600 cm⁻¹ in FTIR spectra confirm the formation of ferrite nanoparticles. Heating of samples to 70.0 °C for 6 hours and addition of Fe₃O₄ nanoparticles (50 µl/ml) at room temperature has same effect i.e. both results in decrease in OCP value. However, decrease in OCP value in case of Fe₃O₄ nanoparticles was small. Values of current first increase and then remain constant with increase in value of potential at room temperature. Continuous stirring of the samples up to 06 hours does not affect its current values. There is no appreciable change in values of current after addition of Fe₃O₄ nanoparticles (50.0 µl/ ml) at room temperature. Heating of samples to 70.0 °C for 6.0 hours leads to decrease in current value. A constant OCP value of 0.778 V in phosphate buffer solution indicates the presence of *Enterobacter aerogenes* pathogenic bacteria in the sample.

Acknowledgement

We are very thankful to DRDO, New Delhi for providing us financial support for this research work.

References

- [1] North Atlantic Treaty Organization. NATO Handbook on the Medical Aspects of NBC Defensive Operations, Part II, Biological NATO Amed, 1996. P-6(B).
- [2] I.Karube, K. Hera, H. Matsuoka, and S.Suzuki, "Amperometric determination of total cholesterol in serum with use of immobilized cholesterol esterase and cholesterol oxidase," *Anal. Chim. Acta.* 1982, 139, 127 –32.
- [3] V. Veldhoven, P. P.Meyhi, and G.P.Mannaerts, "Enzymatic quantitation of cholesterol esters in lipid extracts," *Anal. Biochem.* 1998, 258, 152 – 55.
- [4] B. Shahnaz, S. Tada, T. Kajikawa, T. Ishida, and K.Kawanishi, "Automated fluorimetric determination of cellular cholesterol," *Ann. Clin. Biochem.*, 1998, 345, 665 – 70.
- [5] J. F. Kennedy, In: A.Wiseman, (ed.) Handbook of Enzyme Biotechnology, Chap John Wiley and Sons, New York, 1975.
- [6] E.L. Crowley, C. K.O'Sullivan, and G.G.Guilbault, "Increasing the sensitivity of listeria monocytogenes assays:

- [7] evaluating using ELISA and amperometric detection," *Analyst*, 1999, 124(3), 295-99.
- [8] B. Mirhabibollahi, J. L. Brooks, and R. G. Kroll, "A semi-homogeneous amperometric immunosensor for protein A-bearing *Staphylococcus aureus* in foods," *Appl. Microbiol. Biotechnol.* 1990, 34, 242.
- [9] J. L. Brooks, B. Mirhabibollahi, and R. G. Kroll, "Sensitive enzyme-amplified electrical immunoassay for protein A-bearing *S. Aureus* in food," *Appl. Environ. Microbiol.* 1990, 56, 3278-84.
- [10] N. Nakamura, A. Shigematsu, and T. Matsunaga, "Electrochemical detection of viable bacteria in urine and antibiotic selection," *Biosens. Bioelectron.* 1991, 6, 575.
- [11] J. L. Brook, B. Mirhabibollahi, and R. G. Kroll, "Experimental enzyme linked immunosensor for the detection of *Salmonella* in food," *J. Appl. Bacteriology.* 1992, 73, 189-96.
- [12] H. J. Kim, H. P. Benetto, and M. A. Haqlablab, "A novel liposome based electrochemical biosensor for the detection of haemolytic microorganisms," *Biotechnol. Tech.*, 1995, 9(6), 389-94.
- [13] A. L. Ghindilis, P. Atanasov, P. Wilkins, and E. Wilkins, "A biosensor for *Escherichia coli* based on a potentiometric alternating biosensing (PAB) transducer," *Biosensors Bioelectronics*, 1998, 13, 113-31.
- [14] S. Singh, P. R. Solanki, and B. D. Malhotra, "Covalent immobilization of cholesterol esterase and cholesterol oxidase on polyaniline films for application to cholesterol biosensor," *Anal. Chim. Acta.*, 2006, 568, 126-32.
- [15] J. F. Kennedy *Handbook of Enzyme Technology*, Marcel Dekker, New York, 1985.
- [16] W. E. Lee, H. G. Thomson, J. G. Hall, R. E. Fulton, and J. P. Wong, "Characteristics of the Biochemical detector sensor. Defence Research Establishment Suffield, Canada," Suffield Memorandum No. 1402, 1993, 1-23.
- [17] C. Ercole, M. Del Gallo, M. Pantalone, S. Santucci, L. Mosiello, C. Laconi, and Lepidi. *Sensor Actuators B*, 2002, 4163, 1-5.
- [18] H. Kumar, and R. Rani, "Development of Biosensor for the detection of Biological Warfare Agents: Its Issues & Challenges," *Sci. Progress*, 2013, 96(3), 294-308.
- [19] T. Koutzarova, S. Kolev, C. Ghelev, D. Paneva, and I. Nedkov, "Microstructural study and size control of iron oxide nanoparticles produced by microemulsion technique," *Phys. Stat. Sol. (c)*. 2006, 3(5), 1302-07.
- [20] X. J. Bard, and L. R. Faulkner, *Electrochemical Methods: Fundamentals and Applications*, 2nd ed., Wiley, New York, 2000.
- [21] X. Chen, Y. Wang, J. Zhou, W. Yan, X. Li and J. J. Hu, "Electrochemical impedance immunosensor based on three-dimensionally ordered macroporous gold film," *Anal. Chem.* 2008, 80, 2133-40.
- [22] J. H. Meng, G. Q. Yang, L. M. Yan, and X. Y. Wang, "Synthesis and characterization of magnetic nanometer pigment Fe_3O_4 ," *Dye. Pigments*, 2005, 66, 109-13.
- [23] A. Kaushik, R. Khan, P. R. Solanki, P. Pandey, J. Alam, S. Ahmad, and B. D. Malhotra, "Iron oxide nanoparticles-chitosan composite based glucose biosensor," *Biosens. Bioelectron.* 2008, 24(4), 676-83.
- [24] R. Boistelle, and J. P. Astier, "Crystallization mechanism in solutions," *J. Cryst. Growth*. 1988, 90, 14-30.
- [25] H. K. Moudgil, *A textbook of Physical Chemistry*, 2nd ed., Prentice Hall of India, Pvt. Ltd., New Delhi, 2015, 648-50.
- [25]. J. Wang, Q. Chen, C. Zheng, and B. Hou, "Magnetic-field-induced growth of single-crystalline Fe_3O_4 nanowires," *Adv. Mater.* 2004, 16(2), 137-40.